

## SECTION 1 Normal Chest

### 1 Normal Chest Radiography and Computed Tomography 1

JULIANA BUENO | CHRISTOPHER M. WALKER | JONATHAN H. CHUNG

## SECTION 2 Radiologic Manifestations of Lung Disease

### 2 Consolidation 57

JONATHAN H. CHUNG | CHRISTOPHER M. WALKER

### 3 Atelectasis 71

BRENT P. LITTLE

### 4 Nodules and Masses 91

SARAH T. KURIAN | CHRISTOPHER M. WALKER | JONATHAN H. CHUNG

### 5 Interstitial Patterns 109

JONATHAN H. CHUNG | CHRISTOPHER M. WALKER

### 6 Decreased Lung Density 138

CHRISTOPHER M. WALKER | JONATHAN H. CHUNG

## SECTION 3 Developmental Lung Disease

### 7 Airway and Parenchymal Anomalies 147

JUSTIN T. STOWELL | CHRISTOPHER M. WALKER | JONATHAN H. CHUNG

### 8 Congenital Malformations of the Pulmonary Vessels in Adults 167

BRENT P. LITTLE

## SECTION 4 Pulmonary Infection

### 9 Bacterial Pneumonia 193

STEPHANE L. DESOUCHES | CHRISTOPHER M. WALKER | JONATHAN H. CHUNG

### 10 Pulmonary Tuberculosis 219

KYUNG SOO LEE | YEON JOO JEONG

### 11 Nontuberculous (Atypical) Mycobacterial Infection 241

BRENT P. LITTLE

### 12 Fungal Infections 251

SUZANNE C. BYRNE | REBECCA M. LINDELL | THOMAS E. HARTMAN

### 13 Viruses 273

CHRISTOPHER M. WALKER | JONATHAN H. CHUNG

### 14 Parasites 287

CHRISTOPHER M. WALKER | JONATHAN H. CHUNG

### 15 Human Immunodeficiency Virus Infection 300

CAROL C. WU | JOHN P. LICHTENBERGER | KIRAN BATRA

## SECTION 5 Pulmonary Neoplasms

### 16 Screening for Lung Cancer 317

SUZANNE C. BYRNE | THOMAS E. HARTMAN

### 17 Lung Cancer: Radiologic Manifestations and Diagnosis 324

CAROL C. WU | JEFFREY S. KLEIN

### 18 Pulmonary Carcinoma Staging 341

KYUNG SOO LEE | YEON JOO JEONG

### 19 Neuroendocrine Hyperplasia, Pulmonary Tumorlets, and Carcinoid Tumors 365

STEPHANE L. DESOUCHES | CHRISTOPHER M. WALKER | JONATHAN H. CHUNG

### 20 Pulmonary Hamartoma 376

CHRISTOPHER M. WALKER | JONATHAN H. CHUNG

### 21 Inflammatory Pseudotumor 381

JONATHAN H. CHUNG | CHRISTOPHER M. WALKER

### 22 Pulmonary Metastases 384

STEPHANE L. DESOUCHES | CHRISTOPHER M. WALKER | JONATHAN H. CHUNG

## SECTION 6 Lymphoproliferative Disorders and Leukemia

### 23 Pulmonary Lymphoid Hyperplasia and Lymphoid Interstitial Pneumonia (Lymphocytic Interstitial Pneumonia) 393

JONATHAN H. CHUNG | CHRISTOPHER M. WALKER

### 24 Non-Hodgkin Lymphoma 401

PATRICIA M. DE GROOT | CAROL C. WU | BRETT W. CARTER | KYUNG SOO LEE

### 25 Hodgkin Lymphoma 413

EMILY B. TSAI | CAROL C. WU | VICTORINE V. MUSE | KYUNG SOO LEE

### 26 Leukemia 423

GIRISH S. SHROFF | CAROL C. WU | CHITRA VISWANATHAN | MYLENE T. TRUONG

## SECTION 7 Diffuse Lung Diseases

### 27 Usual Interstitial Pneumonia/Idiopathic Pulmonary Fibrosis 429

JONATHAN H. CHUNG | CHRISTOPHER M. WALKER

### 28 Nonspecific Interstitial Pneumonia 440

JONATHAN H. CHUNG | CHRISTOPHER M. WALKER

### 29 Cryptogenic Organizing Pneumonia/Secondary Organizing Pneumonia 449

JONATHAN H. CHUNG | CHRISTOPHER M. WALKER

- 30 Acute Interstitial Pneumonia 456**  
JONATHAN H. CHUNG | CHRISTOPHER M. WALKER
- 31 Sarcoidosis 461**  
JONATHAN H. CHUNG | CHRISTOPHER M. WALKER
- 32 Hypersensitivity Pneumonitis 478**  
ANDREA L. MAGEE | CHRISTOPHER M. WALKER |  
JONATHAN H. CHUNG
- 33 Pulmonary Langerhans Cell Histiocytosis 494**  
STEPHEN B. HOBBS
- 34 Smoking-Related Interstitial Lung Disease 502**  
STEPHEN B. HOBBS
- 35 Lymphangioliomyomatosis and Tuberos Sclerosis 513**  
NICOLA SVERZELLATI
- 36 Idiopathic Pleuroparenchymal Fibroelastosis 524**  
ROBERT M. DEWITT | STEPHEN K. FRANKEL
- 37 Eosinophilic Lung Diseases 527**  
MELISSA PRICE | CAROL C. WU | MATTHEW D. GILMAN
- 38 Metabolic and Storage Lung Diseases 535**  
CHRISTOPHER M. WALKER | JONATHAN H. CHUNG
- SECTION 8 Connective Tissue Diseases**
- 39 Rheumatoid Arthritis 552**  
STEPHEN B. HOBBS
- 40 Systemic Sclerosis (Scleroderma) 561**  
BRENT P. LITTLE
- 41 Systemic Lupus Erythematosus 565**  
BRENT P. LITTLE
- 42 Polymyositis/Dermatomyositis 571**  
STEPHEN B. HOBBS
- 43 Sjögren Syndrome 576**  
STEPHEN B. HOBBS
- 44 Mixed Connective Tissue Disease 581**  
BRENT P. LITTLE
- 45 Interstitial Pneumonia With Autoimmune Features 585**  
MICHAEL A. KADOCH | JUSTIN M. OLDHAM
- SECTION 9 Vasculitis and Granulomatosis**
- 46 Antineutrophil Cytoplasmic Antibody-Associated Vasculitis 592**  
STEPHANE L. DESOUCHES | CHRISTOPHER M. WALKER |  
JONATHAN H. CHUNG
- 47 Goodpasture Syndrome (Anti-Basement Membrane Antibody Disease) 606**  
JONATHAN H. CHUNG | CHRISTOPHER M. WALKER
- 48 Behçet Disease 611**  
JONATHAN H. CHUNG | CHRISTOPHER M. WALKER
- 49 Takayasu Arteritis 616**  
CHRISTOPHER M. WALKER | JONATHAN H. CHUNG
- SECTION 10 Pulmonary Embolism, Hypertension, and Edema**
- 50 Acute Pulmonary Embolism 622**  
CAROL C. WU | MATTHEW D. GILMAN
- 51 Chronic Pulmonary Thromboembolism 633**  
BRENT P. LITTLE
- 52 Nonthrombotic Pulmonary Embolism 642**  
CHRISTOPHER M. WALKER | JONATHAN H. CHUNG
- 53 Pulmonary Arterial Hypertension 658**  
VEDANT GUPTA | STEPHEN B. HOBBS
- 54 Hydrostatic Pulmonary Edema 674**  
CHRISTOPHER M. WALKER | JONATHAN H. CHUNG
- 55 Permeability Pulmonary Edema 685**  
STEPHEN B. HOBBS
- SECTION 11 Diseases of the Airways**
- 56 Tracheal Diseases 694**  
BRENT P. LITTLE
- 57 Bronchiectasis and Other Bronchial Abnormalities 713**  
BRENT P. LITTLE
- 58 Asthma 733**  
JONATHAN H. CHUNG | CHRISTOPHER M. WALKER
- 59 Bronchiolitis 745**  
SHERIEF GARRANA | CHRISTOPHER M. WALKER |  
JONATHAN H. CHUNG
- 60 Emphysema 765**  
STEPHEN B. HOBBS
- SECTION 12 Inhalational Diseases and Aspiration**
- 61 Asbestos-Related Disease 775**  
STEPHEN B. HOBBS
- 62 Silicosis and Coal Workers' Pneumoconiosis 793**  
STEPHEN B. HOBBS
- 63 Uncommon Pneumoconioses 809**  
STEPHEN B. HOBBS
- 64 Aspiration 822**  
TOMÁS FRANQUET
- SECTION 13 Iatrogenic Lung Disease and Trauma**
- 65 Drug-Induced Lung Disease 836**  
SARAH T. KURIAN | CHRISTOPHER M. WALKER |  
JONATHAN H. CHUNG

**66 Therapeutic Radiation and Radiation-Induced Lung Disease 847**MARCELO F. BENVENISTE | DANIEL R. GOMEZ |  
BRADLEY S. SABLOFF | JEREMY J. ERASMUS**67 Blunt Thoracic Trauma 863**

PHILLIP A. SETRAN | STEVEN L. PRIMACK | CRISTINA S. FUSS

**68 Postoperative Complications 885**

MYLENE T. TRUONG | CAROL C. WU | CHARLES S. WHITE

**69 Chest Radiography in the Intensive Care Unit 907**

ANUPAMA BRIXEY | MATTHEW BENTZ | STEVEN L. PRIMACK

**70 Noninfectious Lung and Stem Cell Transplantation Complications 929**

BRENT P. LITTLE

**SECTION 14 Pleural Disease****71 Pneumothorax 942**

ASHISH GUPTA | JEAN M. SEELY

**72 Pleural Effusion 963**

ASHISH GUPTA | JEAN M. SEELY

**73 Benign Pleural Thickening 988**

CAROL C. WU | JEAN M. SEELY

**74 Pleural Neoplasms 1008**

BRETT W. CARTER | PATRICIA M. DE GROOT | JEAN M. SEELY

**SECTION 15 Mediastinum****75 Pneumomediastinum 1030**

TOMÁS FRANQUET

**76 Mediastinitis 1039**

TOMÁS FRANQUET

**77 Mediastinal Masses 1051**

BRETT W. CARTER

**SECTION 16 Diaphragm and Chest Wall****78 Diaphragm 1070**CHRISTOPHER M. WALKER | JONATHAN H. CHUNG |  
J. DAVID GODWIN**79 Chest Wall 1088**

TOMÁS FRANQUET | JAUME LLAUGER

1

# Normal Chest Radiography and Computed Tomography\*

JULIANA BUENO | CHRISTOPHER M. WALKER | JONATHAN H. CHUNG

## Radiography

### Technique

#### PROJECTIONS

The standard radiographic views for evaluation of the chest are the posteroanterior (PA) and lateral projections with the patient standing; such projections provide the essential requirement for proper three-dimensional (3D) assessment (Fig. 1.1). In patients who are unable to stand, anteroposterior (AP) upright or supine projections offer alternative but considerably less satisfactory views. The AP projection is of inferior quality because of the shorter focal-detector distance, the greater magnification of the heart, and the restricted ability of many such patients to suspend respiration or achieve full inspiration.

#### BASIC RADIOGRAPHIC TECHNIQUES

Diagnostic accuracy in thoracic pathology is related partly to the quality of the radiographic images themselves, and multiple variables require attention.

##### *Patient Positioning and Respiration*

Images are ideally acquired at full inspiration to avoid magnification of the cardiomeastinal silhouette and vascular crowding, which decrease diagnostic capability.

A well-centered x-ray beam, lack of rotation, and exclusion of the scapulae from the field of view are essential for adequate positioning. The distance between the medial ends of the clavicles (anterior structures) and the spinous processes of the thoracic vertebrae (posterior structures) are reliable landmarks to assess position. In a properly centered radiograph the medial ends of the right and left clavicles are equidistant from the spinous processes (Fig. 1.2). The American College of Radiology standards for performance of standard chest radiography in adults specify the use of at least a 72-inch (1.8-m) tube-detector distance for PA radiographs and a minimum of 40 inches in portable radiographs.<sup>1,2</sup>

\*The editors and the publisher would like to thank Drs. Nestor L. Müller and C. Isabela Silva Müller for contributing material on this topic to the prior edition of this work. It has served as the foundation for the current chapter.

##### *Exposure*

Exposure factors should be such that there is faint visualization of the thoracic spine and the intervertebral disks on the PA radiograph so that lung markings behind the heart are clearly visible.<sup>1</sup>

##### *Kilovoltage*

A high-kilovoltage technique (115–150 kVp) should be used for PA and lateral chest radiographs.<sup>1</sup> The high kVp allows better penetration of the mediastinum and shorter exposure times, thus minimizing cardiac motion artifacts and providing sharper outline of the pulmonary and mediastinal structures.<sup>1</sup>

#### IMAGE ACQUISITION

Conventional screen-film radiography has a number of limitations and therefore has been replaced by computed radiography (CR) and digital radiography (DR).

The process of acquisition, transmission, display, and storage of digital images has many advantages over conventional screen-film systems,<sup>3,4</sup> and it is widely used as the primary technology in conventional radiographic studies. A potential disadvantage of CR and DR is that patients may receive unnecessarily high radiation doses, which may not be detected because they do not result in perceivable alterations in image quality. The wider latitude of digital systems allows them to be used under a much broader range of exposure conditions and makes them an ideal choice for applications in which exposure is highly variable or difficult to control, such as bedside radiography. This results in a reproducible quality and considerable decrease in the repeat rate for bedside chest radiographs when using CR, compared with screen-film radiography.<sup>5</sup>

Two main types of digital systems are available commercially: systems based on photostimulable storage phosphor image receptors, known as CR, and systems based on flat-panel x-ray detectors or array of detectors that directly capture the radiographic image, known as DR.

##### *Computed Radiography*

CR (storage phosphor radiography) involves the use of a reusable photostimulable phosphor plate rather than film to record the image. Plates coated with the phosphor are loaded into special cassettes that are outwardly similar to screen-film cassettes. During exposure the receptor stores the x-ray energy and is then scanned by a laser beam, which results in the creation of visible or infrared

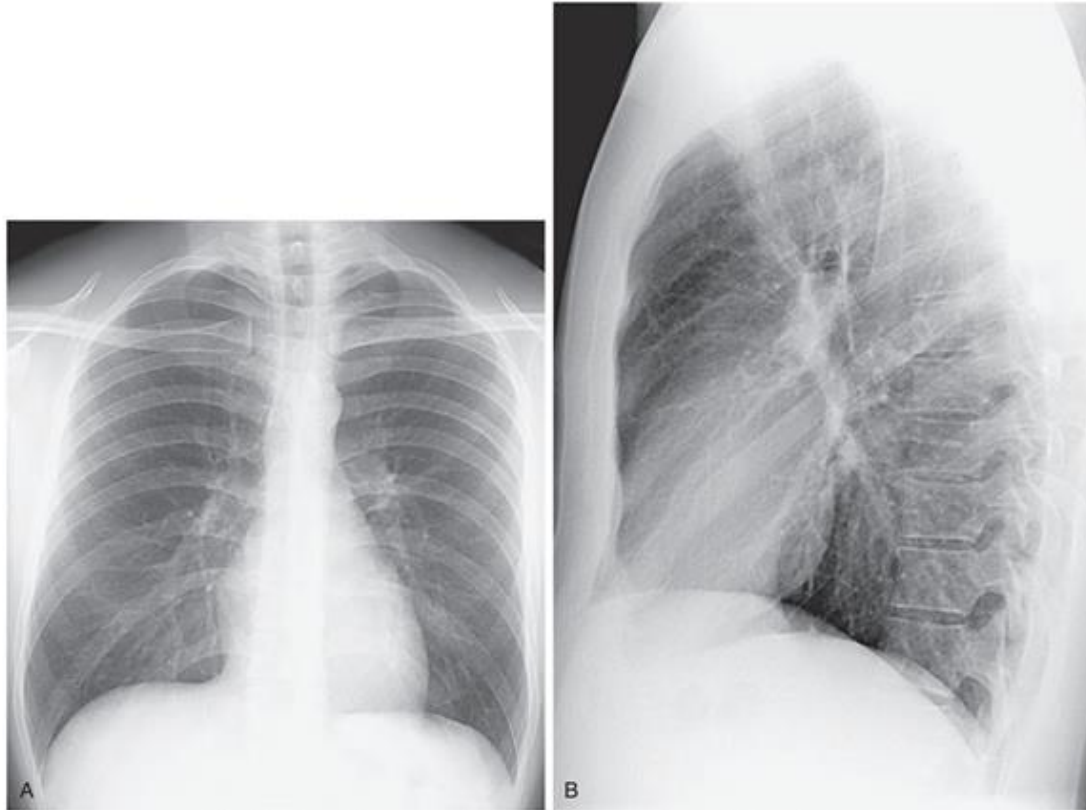


**Fig. 1.1** Normal chest radiograph. (A) Posteroanterior projection. (B) Lateral projection.



**Fig. 1.2** Properly centered chest radiograph. A view from a frontal radiograph shows that the medial ends of the right and left clavicles (highlighted in black) are equidistant to the spinous process (arrow) of the vertebra at the same level, thus indicating that the radiograph is properly centered.

radiation, the intensity of which corresponds to the absorbed x-ray energy. The resultant luminescence is measured and recorded digitally.<sup>6</sup>

#### Digital Radiography

DR uses a flat-panel x-ray detector or an array of detectors to directly capture the radiographic image numerically, thus

eliminating the step of reading out the detector. The detectors in DR are selenium based and provide the additional advantage of having considerably greater quantum efficiency than conventional screen-film systems and photostimulable phosphor detectors do,<sup>7,8</sup> which results in an image quality superior to that of screen-film systems and existing storage phosphor detectors at a comparable or lower radiation dose.<sup>9</sup>

## Normal Anatomy of the Chest

### AIRWAYS

#### Trachea and Bronchi

The trachea is a midline structure, and the tracheal walls are parallel except on the left side just above the bifurcation, where the aorta commonly causes a smooth indentation (Fig. 1.3). The trachea measures 10 to 12 cm in length and has 16 to 20 C-shaped cartilage rings on its lateral and anterior aspects and a fibromuscular posterior margin. Calcification of the cartilage rings is a common normal finding in patients older than 40 years, particularly women, but it is seldom evident on radiographs (Fig. 1.4). The upper limits of normal for coronal and sagittal

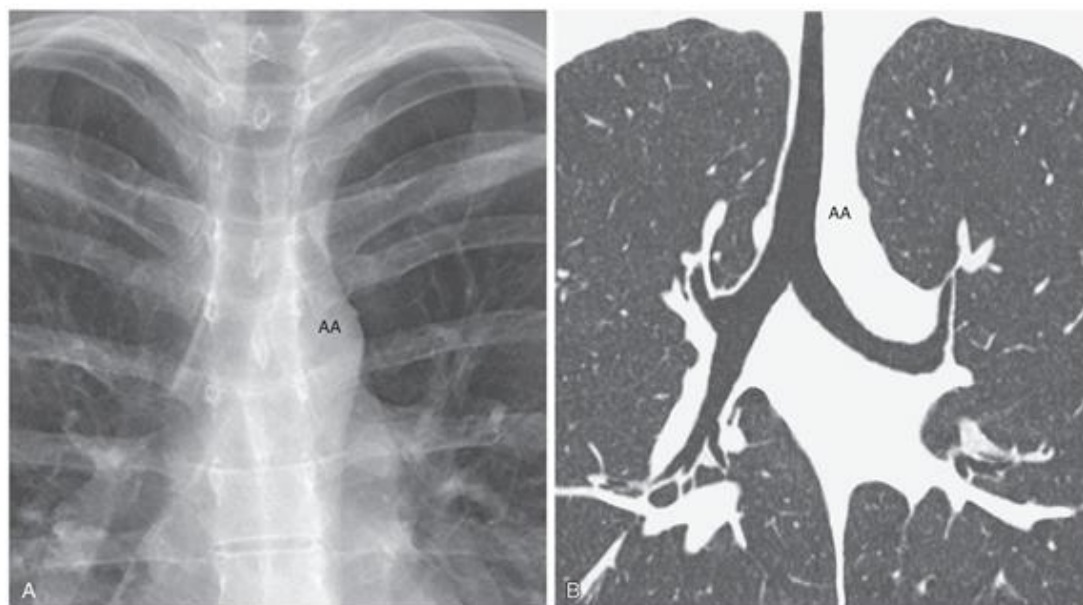


**Fig. 1.3** Normal trachea and main bronchi. (A) Frontal radiograph shows that the tracheal air column is fairly straight and located in the midline except at the level of the aortic arch (AA), where the trachea is indented and may be slightly deviated to the right. The trachea divides into a short right main bronchus and a longer and more horizontal left main bronchus. (B) Coronal reformatted image from a CT scan demonstrating the normal anatomy of the trachea, the slight indentation at the level of the aortic arch (AA), and the main bronchi. Approximately 2 cm after its origin, the right main bronchus branches into the right upper lobe bronchus and the bronchus intermedius.

diameters of the trachea in men are 25 and 27 mm, respectively; in women, they are 21 and 23 mm, respectively.<sup>10</sup> The lower limit of normal for both dimensions is 13 mm in men and 10 mm in women.<sup>10</sup>

The trachea divides into the left and right main bronchi at the carina, at approximately the level of the fifth thoracic vertebra. The subcarinal angle ranges widely from 35 to 90 degrees (mean, 61 degrees)<sup>11</sup>; thus routine measurement of this angle has no diagnostic value.

The right main bronchus measures approximately 2 cm in length and has a more vertical course than the left main bronchus does (see Fig. 1.3). It divides into the right upper lobe bronchus and the bronchus intermedius. The bronchus intermedius continues distally for 3 to 4 cm from the takeoff of the right upper lobe bronchus and then bifurcates into bronchi to the middle and lower lobes. The left main bronchus is approximately 5 cm in length and divides into the left upper and lower lobe bronchi.

The lobar bronchi branch into segmental bronchi. Segmental bronchi are visible on chest radiographs only when they are seen end-on as ring shadows or when they are abnormally thickened. The most commonly seen segmental bronchi on a chest radiograph are the anterior segmental bronchi of the upper lobes; seen as ring shadows adjacent to the accompanying segmental pulmonary artery (Fig. 1.5).

#### KEY POINTS: TRACHEA

- Normal diameter in men is 13–27 mm.
- Normal diameter in women is 10–23 mm.
- The tracheal cartilages are C shaped and spare the posterior tracheal wall, which is membranous.

## PULMONARY ARTERIAL AND VENOUS CIRCULATION

### Pulmonary Arteries

The pulmonary trunk or main pulmonary artery originates in the mediastinum at the pulmonary valve and extends cranially and slightly to the left for 4 to 5 cm before bifurcating within the pericardium into the shorter left and longer right pulmonary arteries (Fig. 1.6). The left pulmonary artery continues until it reaches the hilum, where it arches over the left main bronchus and gives off the left upper lobe and interlobar arteries, from which segmental and subsegmental branches arise. The left interlobar artery lies posterolateral to the upper lobe bronchus.

The right pulmonary artery courses behind the ascending aorta before dividing in front of the right main bronchus into ascending (truncus anterior) and descending (interlobar) branches.

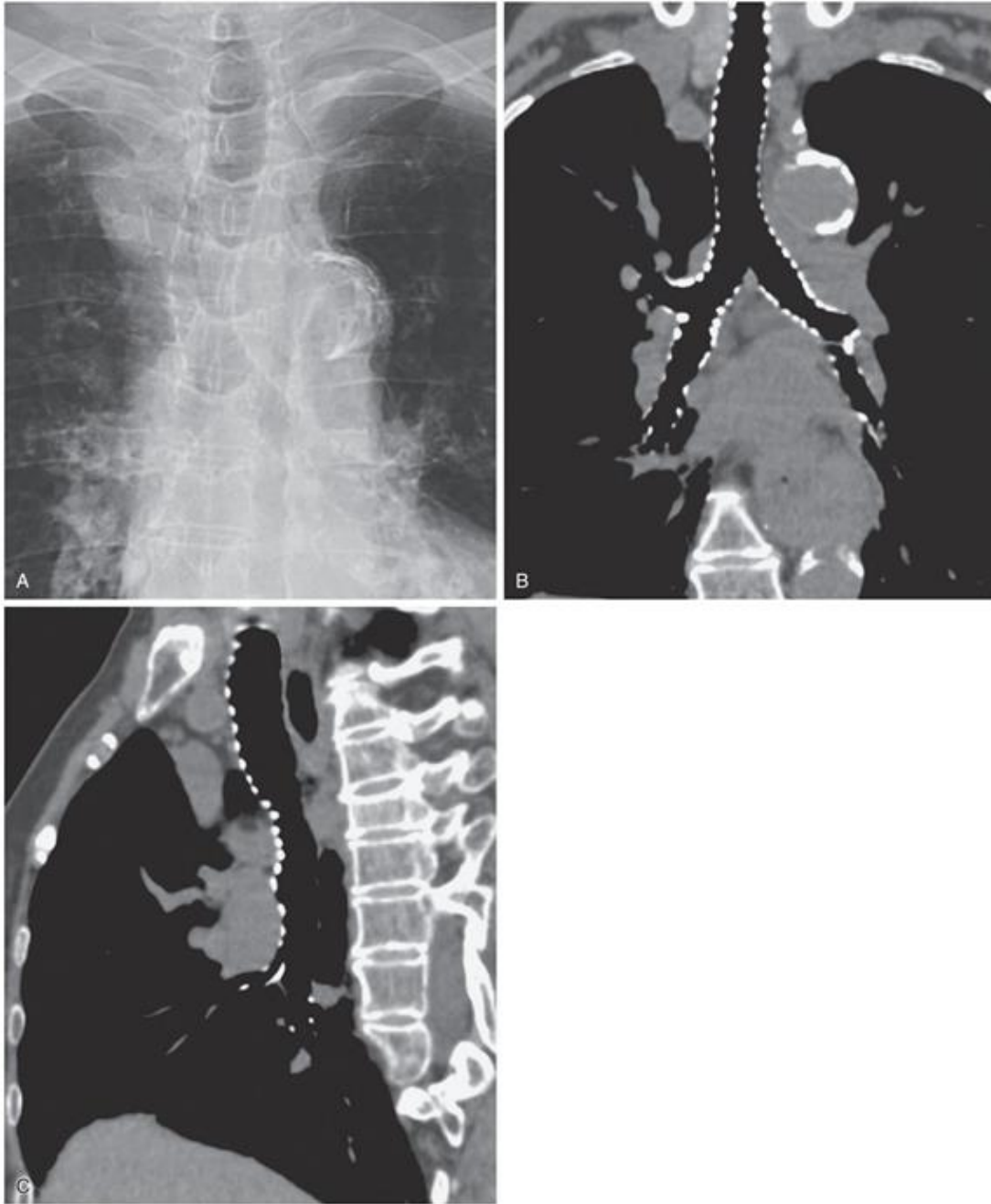


**Fig. 1.4** Tracheal and bronchial wall calcification. A magnified view from a posteroanterior chest radiograph (A) in an elderly patient shows calcification of the tracheal and bronchial walls. Coronal (B) and sagittal (C) reformatted images from a CT scan show the extent of tracheal and bronchial calcification. Airway wall calcification is a normal finding in elderly patients.

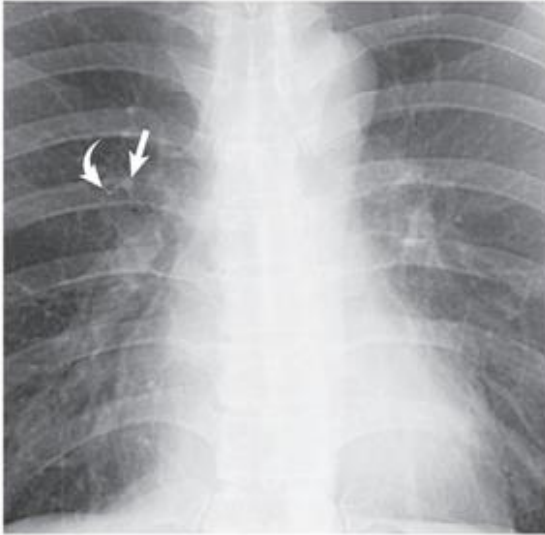


**Fig. 1.5** Anterior segmental bronchus of the right upper lobe seen end-on. A view from a frontal radiograph shows a ring shadow (*curved arrow*) corresponding to the anterior segmental bronchus of the right upper lobe seen end-on and the adjacent anterior segmental pulmonary artery (*straight arrow*). The outer diameter of the bronchus on the upright chest radiograph is slightly larger than that of the adjacent artery.

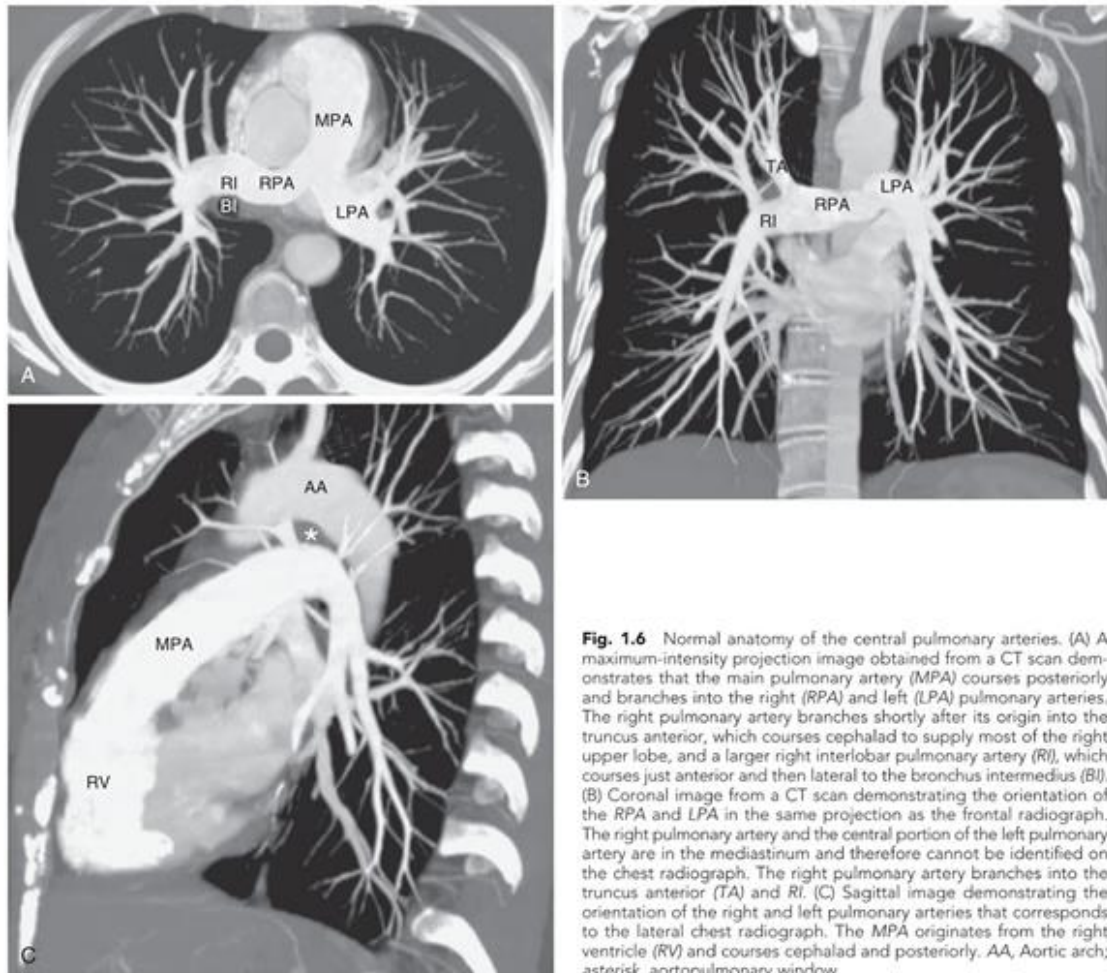


**Fig. 1.6** Normal anatomy of the central pulmonary arteries. (A) A maximum-intensity projection image obtained from a CT scan demonstrates that the main pulmonary artery (MPA) courses posteriorly and branches into the right (RPA) and left (LPA) pulmonary arteries. The right pulmonary artery branches shortly after its origin into the truncus anterior, which courses cephalad to supply most of the right upper lobe, and a larger right interlobar pulmonary artery (RI), which courses just anterior and then lateral to the bronchus intermedius (BI). (B) Coronal image from a CT scan demonstrating the orientation of the RPA and LPA in the same projection as the frontal radiograph. The right pulmonary artery and the central portion of the left pulmonary artery are in the mediastinum and therefore cannot be identified on the chest radiograph. The right pulmonary artery branches into the truncus anterior (TA) and RI. (C) Sagittal image demonstrating the orientation of the right and left pulmonary arteries that corresponds to the lateral chest radiograph. The MPA originates from the right ventricle (RV) and courses cephalad and posteriorly. AA, Aortic arch; asterisk, aortopulmonary window.

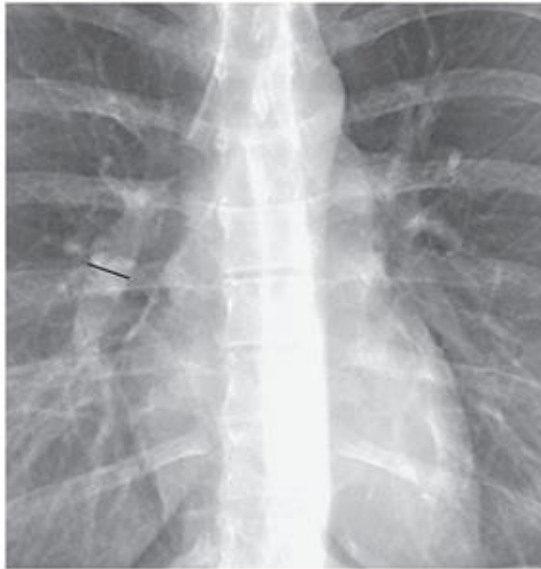


**Fig. 1.7** Normal right interlobar artery visualized on a frontal chest radiograph. The upper limit of normal of the transverse diameter of the interlobar artery measured from its lateral aspect to the air column of the bronchus intermedius (black bar) is 16 mm in men and 15 mm in women.

Measurements of pulmonary arterial diameter can be helpful in the assessment of pulmonary vascular disease, although in conventional radiography, it is limited to the measurement of the right interlobar artery. The upper limit of normal of the transverse diameter of the right interlobar artery (measured from its lateral aspect to the air column of the bronchus intermedius) is 16 mm in men and 15 mm in women (Fig. 1.7).<sup>12</sup> Dilatation of the interlobar pulmonary artery may result from increased pressure (e.g., pulmonary arterial hypertension), increased flow (e.g., left-to-right shunts), or aneurysm formation (e.g., Behçet disease) (Fig. 1.8).

#### KEY POINTS: PULMONARY ARTERIES

- The pulmonary trunk or main pulmonary artery is not normally visualized on radiography in adults.
- Normal diameter of the right interlobar pulmonary artery is <16 mm.

#### Pulmonary Veins

The pulmonary veins arise from venules that drain the alveolar capillaries and the capillary network of the pleura. In contrast to the pulmonary arteries, they are not associated with the airways. Although their final course is variable, there are usually two main superior and two main inferior vessels, the former draining the middle and upper lobes on the right and the upper lobe on the left and the latter draining the lower lobes (Fig. 1.9).

#### PULMONARY HILA

The anatomic structures rendering the hila visible on radiographs are primarily the pulmonary arteries and veins, with lesser



**Fig. 1.8** Enlarged central pulmonary arteries from severe pulmonary arterial hypertension. A frontal radiograph shows markedly enlarged central pulmonary arteries.

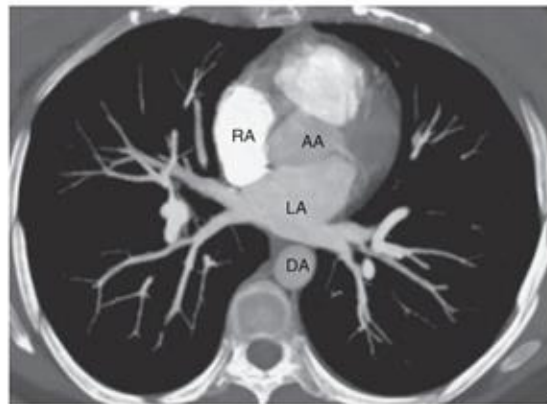


**Fig. 1.9** Inferior pulmonary veins. A maximum-intensity projection image obtained from a CT scan shows two main right and left inferior pulmonary veins as they drain into the left atrium (LA). AA, Ascending aorta; DA, descending aorta; RA, right atrium.

contributions from the bronchial walls, surrounding connective tissue, and lymph nodes (Fig. 1.10).

On a PA radiograph the main shadow of the right hilum is formed by the vertically oriented interlobar artery. Right hilar structures immediately cephalad to the interlobar artery include the ascending pulmonary artery (truncus anterior) and superior pulmonary vein (Fig. 1.11). The end-on opacity and radiolucency of the contiguous anterior (and occasionally posterior) segmental artery and bronchus can be identified in approximately 80% of normal individuals (see Fig. 1.5).<sup>13</sup>

On the left the upper hilar opacity is formed by the distal left pulmonary artery, the proximal portion of the left interlobar